Ruthenium Thioether Chemistry: The Synthesis and Structure of a Host–Guest Complex $[Ru([9]aneS_3)_2][BPh_4]_2{\cdot}2Me_2SO$, and of $[Ru([9]aneS_3)_2][BPh_4]_2{\cdot}2MeNO_2$ and $[Ru([18]aneS_6)][BPh_4]_2$ ($[9]aneS_3$ = 1,4,7-trithiacyclononane, $[18]aneS_6$ = 1,4,7,10,13,16-hexathiacyclo-octadecane)†

Michael N. Bell, Alexander J. Blake, Alan J. Holder, Timothy I. Hyde, and Martin Schröder *
Department of Chemistry, University of Edinburgh, West Mains Road, Edinburgh EH9 3JJ, Scotland

Reaction of $[\{RuCl_2(arene)\}_2]$ (arene = C_6H_6, C_6Me_6, or 4-$MeC_6H_4Pr^i$) with four molar equivalents of 1,4,7-trithiacyclononane ($[9]aneS_3$) in MeOH at 293 K affords a colourless or pale yellow solution. Addition of $NaBPh_4$ gives $[Ru([9]aneS_3)_2][BPh_4]_2$ which can be recrystallised from Me_2SO, $MeNO_2$, or MeCN. The complex $[Ru([9]aneS_3)_2][BPh_4]_2{\cdot}2Me_2SO$ crystallises in the monoclinic space group $P2_1/c$ with a = 14.134(3), b = 11.096 3(19), c = 19.743(4) Å, β = 94.497(16)°, and Z = 2. The single crystal X-ray structure of the complex shows a centrosymmetric cation with homoleptic thioether co-ordination to an octahedral Ru^{II} ion. Each macrocycle is bound facially to the metal centre, Ru–S(1) 2.327 2(14), Ru–S(4) 2.335 7(14), Ru–S(7) 2.333 1(14) Å. Two molecules of Me_2SO are associated with each $[Ru([9]aneS_3)_2]^{2+}$ cation; these interact with the rear cavities of the co-ordinated trithia macrocycles to form a host/guest-type interaction, with the oxygen atoms involved in hydrogen bonding with the methylene protons of $[9]aneS_3$, O $\cdots$ H 2.201(8), 2.419(8), 2.790(8), and 3.291(8) Å. The Me_2SO molecules in $[Ru([9]aneS_3)_2][BPh_4]_2{\cdot}2Me_2SO$ can be replaced by MeCN or $MeNO_2$ by recrystallisation of the complex from these solvents. The complex $[Ru([9]aneS_3)_2][BPh_4]_2{\cdot}2MeNO_2$ crystallises in the monoclinic space group $P2_1/n$ with a = 11.200(5), b = 18.247(13), c = 14.323(17) Å, β = 90.78(4)°, and Z = 2. The single crystal X-ray structure of this species, however, shows that there is no secondary interaction between the two $MeNO_2$ molecules and the complex cation, the closest contact between the methylene protons and the oxygen atoms of $MeNO_2$ being over 3.5 Å. The complex cation $[Ru([9]aneS_3)_2]^{2+}$ shows a quasi-reversible oxidation at platinum electrodes in MeCN at $E_{\frac{1}{2}}$ = +1.41 V *vs.* ferrocene–ferrocenium indicating that Ru^{II} is highly stabilised by RuS_6 co-ordination. Reaction of $RuCl_3{\cdot}3H_2O$ with one molar equivalent of 1,4,7,10,13,16-hexathiacyclo-octadecane ($[18]aneS_6$) in refluxing dimethylformamide (dmf)–methanol affords $[Ru([18]aneS_6)]Cl_2$ as a white precipitate. Dissolution of this product in hot water followed by addition of an excess of $NaBPh_4$ yields $[Ru([18]aneS_6)][BPh_4]_2$ which crystallises in the monoclinic space group $P2_1/c$, with a = 12.801(4), b = 10.663(3), c = 20.036(9) Å, β = 109.09(3)°, and Z = 2. The single crystal X-ray structure of the complex shows a centrosymmetric cation with hexathia co-ordination of the macrocycle to Ru^{II} in a *meso* configuration, Ru–S(1) 2.322 2(23), Ru–S(4) 2.332 6(25), Ru–S(7) 2.337 2(23) Å, and confirms that $[18]aneS_6$ can readily fully encapsulate a relatively large cation such as Ru^{II}. The oxidative chemistry of $[Ru([9]aneS_3)_2]^{2+}$ and $[Ru([18]aneS_6)]^{2+}$ is discussed.

The trithia macrocyclic ligand 1,4,7-trithiacyclononane ($[9]aneS_3$) tends to co-ordinate to transition-metal centres in a facial manner as a formal six-electron donor.[1] Thus, bis-(sandwich) complexes of the type $[M([9]aneS_3)_2]^{x+}$ have now been reported for a wide range of transition-metal centres.[1,2] We report herein the synthesis and structure of the homoleptic thioether ruthenium(II) complex $[Ru([9]aneS_3)_2]^{2+}$, which shows an unusual host–guest interaction between the co-ordinated thioether ring and two Me_2SO solvate molecules. This work has been the subject of a preliminary communication.[3,4]

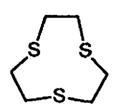

$[9]aneS_3$

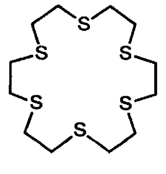

$[18]aneS_6$

The related hexathia ligand 1,4,7,10,13,16-hexathiacyclo-octadecane ($[18]aneS_6$), the thioether analogue of the oxo-polyether 18-crown-6, has been found to encapsulate a range of first-row transition-metal centres.[5] The only second- and third-row complexes of $[18]aneS_6$ of type $[M([18]aneS_6)]^{x+}$ reported thus far are of $Pd^{II,III}$, $Pt^{II,III}$,[1,6,7] Ag,[8] and Au.[9] All these complexes, however, show distortions from regular octahedral geometry due to electronic factors; for example, the

---

† *Supplementary data available:* see Instructions for Authors, *J. Chem. Soc., Dalton Trans.*, 1990, Issue 1, pp. xix—xxii.

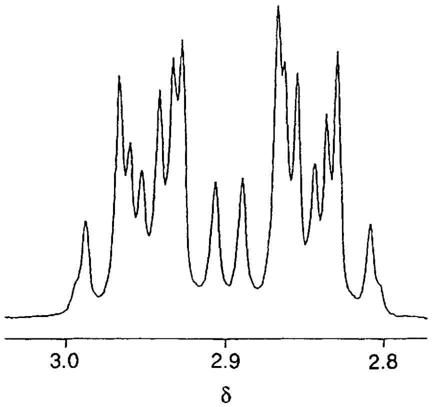

Figure 1. Proton n.m.r. spectrum (360 MHz, CD_3CN, 298 K) of $[Ru([9]aneS_3)_2]^{2+}$

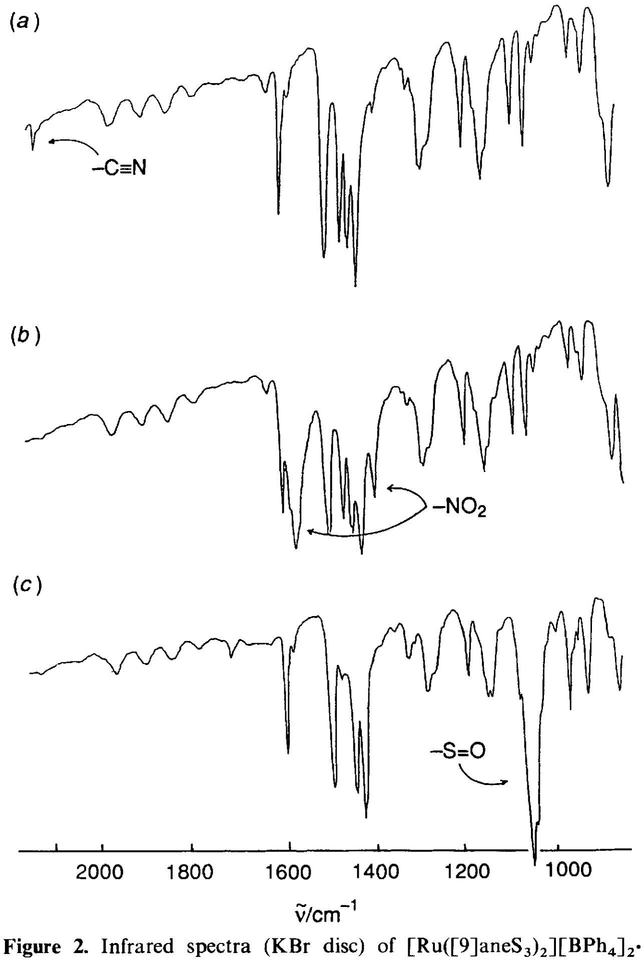

Figure 2. Infrared spectra (KBr disc) of $[Ru([9]aneS_3)_2][BPh_4]_2$·2(solvate); solvate = (*a*) MeCN, (*b*) $MeNO_2$, (*c*) Me_2SO

$[Pd([18]aneS_6)]^{2+/3+}$ cations both show tetragonally elongated stereochemistries consistent with metal d^8 and d^7 configurations respectively.[6,7] The encapsulation of second- and third-row metal ions is inhibited by the kinetic inertness of these metal ions relative to first-row ions. In principle, therefore, the synthesis of macrocyclic complexes of these metal ions may present difficulties. We were interested in ascertaining whether $[18]aneS_6$ is capable of fully encapsulating an inert d^6 metal ion octahedrally. We report herein the facile synthesis of $[Ru([18]aneS_6)]^{2+}$ directly from $RuCl_3·3H_2O$ and the crystal structure of its tetraphenylborate salt.

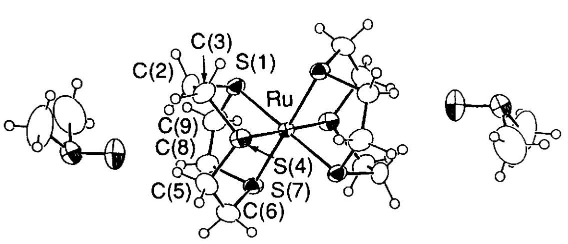

Figure 3. Single crystal *X*-ray structure of $[Ru([9]aneS_3)_2]^{2+}·2Me_2SO$ with atom numbering scheme adopted; 30% probability level used for ellipsoids

Results and Discussion

Reaction of the orange-yellow complexes $[\{RuCl_2(arene)\}_2]$ (arene = C_6H_6, C_6Me_6, or $4\text{-}MeC_6H_4Pr^i$) with four molar equivalents of $[9]aneS_3$ in MeOH at room temperature affords a colourless or pale yellow solution. The rate of reaction varies as a function of arene used: with C_6H_6 the reaction is complete after 10 min, while for $4\text{-}MeC_6H_4Pr^i$ and C_6Me_6 reaction takes 0.5 and 1.5 h respectively for completion at room temperature. Addition of $NaBPh_4$ to the resulting methanolic solution affords a white product which can be recrystallised from polar solvents such as Me_2SO, $MeNO_2$, or MeCN to give an overall yield of up to 70%. The ^1H n.m.r. spectrum of the product confirms the absence of co-ordinated arene and shows an ABCD pattern for the protons of co-ordinated $[9]aneS_3$ (Figure 1) as observed for related sandwich complexes of type $[M([9]aneS_3)_2]^{x+}$.[10–12] The presence of symmetrically bound $[9]aneS_3$ was confirmed from the ^{13}C n.m.r. spectrum which showed only one resonance at 33.34 p.p.m. for the methylene carbon centres of co-ordinated $[9]aneS_3$. Fast-atom bombardment (f.a.b.) mass spectroscopy of the product gives molecular-ion peaks corresponding to $[Ru([9]aneS_3)_2][BPh_4]_2$. However, n.m.r. and i.r. spectroscopy (Figure 2) together with elemental analysis indicated the presence of two molecules of solvate (Me_2SO, $MeNO_2$, or MeCN) per Ru^{II} cation. This solvent of crystallisation was retained after drying the complex *in vacuo* at room temperature, but could be removed at higher temperatures. In order to confirm homoleptic thioether co-ordination about Ru^{II} and to ascertain the interaction of the cation with the solvate molecules in the solid state, crystal structure determinations of two of these products were undertaken.

The single crystal *X*-ray structure of $[Ru([9]aneS_3)_2][BPh_4]_2·2Me_2SO$ shows a centrosymmetric cation with the Ru atom lying on an inversion centre. Homoleptic thioether co-ordination to the octahedral Ru^{II} ion is confirmed with each macrocycle bound facially to the metal centre, Ru–S(1) 2.327 2(14), Ru–S(4) 2.335 7(14), Ru–S(7) 2.333 1(14) Å, S(1)–Ru–S(4) 87.87(5), S(1)–Ru–S(7) 88.09(5), S(4)–R–S(7) 88.26(5)° (Figure 3). The complex $[Ru([9]aneS_3)_2]^{2+}$ represents the first example of homoleptic hexathia ether co-ordination to ruthenium and is therefore an important compound with which to probe the electronic properties of thioether ligands in general. Two molecules of Me_2SO are present per Ru^{II} cation and are well ordered and fully occupied. Remarkably, the oxygen atoms of the solvate are orientated towards the rear cavity of the co-ordinated trithia macrocycles producing close O···H intermolecular contacts, O···H(3MA) 2.201(8), O···H(6MA) 2.419(8), O···H(9MA) 2.790(8), O···H(5MA) 3.291(8) Å. The oxygen donors of the Me_2SO are markedly closer to S(7) than to S(1) or S(4). This supplementary interaction is particularly intriguing since it suggests that *inclusion* of Me_2SO is occurring into the rear cone/cavity formed by $[9]aneS_3$ on co-ordination to the metal centre (Figure 4).

The Me_2SO molecules in $[Ru([9]aneS_3)_2][BPh_4]_2·2Me_2SO$

Table 1. M^{II}–M^{III} redox couples ($E_{\frac{1}{2}}$ *vs* ferrocene–ferrocenium) for sandwich complexes $[M([9]aneS_3)_2]^{2+/3+}$ in MeCN at platinum electrodes[1]

Fe^{II}–Fe^{III}	+0.98[12,13]	Co^{II}–Co^{III}	−0.013[11,12]	Ni^{II}–Ni^{III}	+0.97[12]
Ru^{II}–Ru^{III}	+1.41[3,a]	Rh^{II}–Rh^{III}	−0.71[10]	Pd^{II}–Pd^{III}	+0.605[16]
Os^{II}–Os^{III}	+1.16[14]	Ir^{II}–Ir^{III}	−1.38[15,b]	Pt^{II}–Pt^{III}	+0.39[17,c]

[a] This work. [b] Irreversible. [c] Overlapping Pt^{II}–Pt^{III} and Pt^{III}–Pt^{IV} couples.

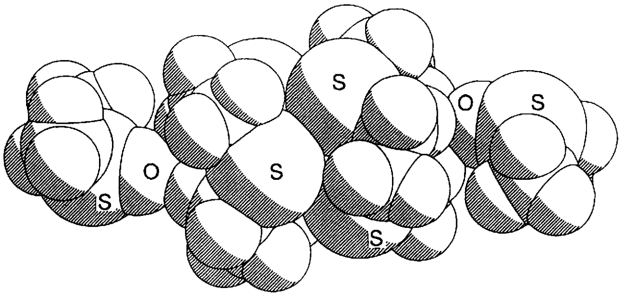

Figure 4. Space-filling diagram of $[Ru([9]aneS_3)_2]^{2+}\cdot Me_2SO$

can be replaced by CH_3CN or $MeNO_2$ by recrystallisation of the complex from these solvents. The single-crystal *X*-ray structure of $[Ru([9]aneS_3)_2][BPh_4]_2\cdot 2MeNO_2$, however, shows that there are no secondary interactions between the two $MeNO_2$ molecules and the complex cation, with the closest contact between the methylene protons and the oxygen atoms of $MeNO_2$ being over 3.5 Å. The solvate molecules are severely disordered and it was not possible to freely refine their atomic co-ordinates. A rigid $MeNO_2$ molecule was introduced in two alternative positions and these were allowed to refine, but maintaining a common central nitrogen position. This lack of close contacts between $MeNO_2$ and the cation is consistent with the disorder of the solvate and the tendency for the crystal to decay. A tentative explanation as to why the oxygen atoms of $MeNO_2$ do not project into the co-ordinated macrocyclic cone is that $MeNO_2$ is planar with two polar oxygen atoms and therefore sterically cannot orientate itself into a suitable position for close interaction. Not surprisingly, the structure of the $[Ru([9]aneS_3)_2]^{2+}$ cation in this complex does not differ significantly from that observed in $[Ru([9]aneS_3)_2][BPh_4]_2\cdot 2Me_2SO$.

The complex $[Ru([9]aneS_3)_2][PF_6]_2$ is electrochemically inactive between −2.2 and +1.3 V, and shows a quasi-reversible oxidation at platinum electrodes in MeCN (0.1 mol dm^{-3} $NBu^n{}_4PF_6$) at $E_{\frac{1}{2}} = 1.41$ V *vs.* ferrocene–ferrocenium ($\Delta E = 95$ mV, scan rate = 100 mV s^{-1}). We tentatively assign this oxidation to a Ru^{II}–Ru^{III} redox couple, although oxidation of the ligand at these potentials cannot be ruled out entirely. An irreversible reduction is also observed at $E_{pc} = -2.25$ V; this leads to the breakdown of the complex, presumably *via* an unstable Ru^I intermediate, with release of free ligand which can be detected on the return scan as an irreversible oxidation at +0.98 V. The high redox stability of $[Ru([9]aneS_3)_2]^{2+}$ is remarkable and reflects the stereochemical and electronic features of octahedral, homoleptic thioether co-ordination at d^6 Ru^{II} (Table 1).

Reaction of $RuCl_3\cdot 3H_2O$ with one molar equivalent of $[18]aneS_6$ in refluxing dimethylformamide (dmf)–methanol affords $[Ru([18]aneS_6)]Cl_2$ as a white precipitate. Dissolution of this product in hot water followed by addition of an excess of NH_4PF_6 or $NaBPh_4$ yields $[Ru([18]aneS_6)][PF_6]_2$ or $[Ru([18]aneS_6)][BPh_4]_2$ respectively. Alternatively, the latter complex can be prepared directly from $RuCl_3\cdot 3H_2O$ by treatment with $[18]aneS_6$ in the presence of $NaBPh_4$ in refluxing dmf–MeOH–H_2O. The ^1H and ^{13}C n.m.r. spectra of $[Ru([18]aneS_6)]^{2+}$ confirm symmetric binding of the hexathia ligand to Ru^{II}. The single crystal *X*-ray structure of $[Ru([18]aneS_6)][BPh_4]_2$ shows (Figure 5) a centrosymmetric cation with hexathia co-ordination of the macrocycle to Ru^{II} in a *meso* configuration, Ru–S(1) 2.322 2(23), Ru–S(4) 2.332 6(25), Ru–S(7) 2.337 2(23) Å, S(1)–Ru–S(4) 88.67(8), S(1)–Ru–S(7) 91.61(8), S(4)–Ru–S(7) 88.54(8)°. Most importantly, therefore, the bond lengths and angles in $[Ru([18]aneS_6)]^{2+}$ are very similar to those of $[Ru([9]aneS_3)_2]^{2+}$ showing that Ru^{II} fits $[18]aneS_6$ without any apparent distortion of metal co-ordination or ligand geometry. The difficulties in the preparation of second- and third-row complexes of $[18]aneS_6$ are therefore related to the kinetic inertness of these metal ions and the insolubility of intermediate products rather than any inherent mis-match between the metal ion and the macrocyclic cavity.

Oxidation of $[Ru([18]aneS_6)][PF_6]_2$ with $NOBF_4$ in concentrated H_2SO_4 affords a blue-green solution of $[Ru([18]aneS_6)]^{3+}$ [$\lambda_{max.}$ ($\varepsilon_{max.}$) = 742 (sh) (1 260), 680 (1 360), 474 (207), 419 (187), and 354 nm (951 dm^3 mol^{-1} cm^{-1})], which shows an e.s.r. spectrum (77 K, frozen glass) with $g_\perp = 2.328$, $g_\parallel = 1.942$. These solutions decompose slowly over a number of days at room temperature. Similar data can be obtained for the less stable blue cation, $[Ru([9]aneS_3)_2]^{3+}$, $g_\perp = 2.293$, $g_\parallel = 1.863$, for the green $[Fe([9]aneS_3)_2]^{3+}$,[12,13] $g_\perp = 2.328$, $g_\parallel = 1.942$, and the blue $[Os([9]aneS_3)_2]^{3+}$, $g_\perp = 2.358$, $g_\parallel = 1.860$.[14] The oxidised products of $[9]aneS_3$ with Fe^{III}, Ru^{III}, and Os^{III} are particularly unstable in CH_3CN; thus, electrochemically generated solutions of the 3+ cations decompose readily at room temperature. The stabilisation of 3+ cations in highly acidic oxidising media (H_2SO_4 or $HClO_4$) has been described previously and is linked to inhibition of metal-mediated ring-opening reactions to afford vinyl thioether products.[18] The above data are, however, consistent with the formation of Ru^{III} $t_{2g}{}^5$ metal centres,[19] although significant oxidation at the ligand sites cannot be discounted. It should be noted that the oxidation potential for $[Ru([9]aneS_3)_2]^{2+}$ is more anodic than for the metal-free ligand which shows an irreversible oxidation at $E_a = 0.98$ V *vs.* ferrocene–ferrocenium.[1]

Experimental

Infrared spectra were measured as Nujol mulls, KBr, and CsI discs using a Perkin-Elmer 598 spectrometer over the range 200—4 000 cm^{-1}. U.v.–visible spectra were measured in quartz cells using Perkin-Elmer Lambda 9 and Pye Unicam SP8-400 spectrophotometers. Microanalyses were performed by the Edinburgh University Chemistry Department microanalytical service. E.s.r. spectra were recorded as solids or as frozen glasses down to 77 K using a Bruker ER200D *X*-band spectrometer. Electrochemical measurements were performed on a Bruker E310 Universal Modular Polarograph. All readings were taken using a three-electrode potentiostatic system in acetonitrile containing 0.1 mol dm^{-3} $NBu^n{}_4PF_6$ or $NBu^n{}_4BF_4$ as supporting electrolyte. Cyclic voltammetric measurements were carried out using a double platinum electrode and an Ag–AgCl reference electrode. All potentials are quoted *vs.* ferrocene–ferrocenium. Mass spectra were run by electron impact on a Kratos MS 902 and by fast atom bombardment on a Kratos MS 50TC spectrometer. Proton and ^{13}C n.m.r. spectra were

Table 2. Bond lengths (Å), angles and torsion angles (°) with estimated standard deviations (e.s.d.s) for $[Ru([9]aneS_3)_2][BPh_4]_2 \cdot 2Me_2SO$ *

Ru–S(1)	2.328 5(12)	C(5M)–C(6M)	1.511(8)
Ru–S(4)	2.334 3(13)	C(6M)–S(7)	1.837(6)
Ru–S(7)	2.333 5(12)	S(7)–C(8M)	1.827(6)
S(1)–C(2M)	1.812(6)	C(8M)–C(9M)	1.521(8)
S(1)–C(9M)	1.834(6)	S–O	1.495(5)
C(2M)–C(3M)	1.506(8)	S–C(1)	1.734(9)
C(3M)–S(4)	1.832(6)	S–C(2)	1.728(9)
S(4)–C(5M)	1.820(6)		
S(1)–Ru–S(4)	87.82(4)	S(4)–C(5M)–C(6M)	114.6(4)
S(1)–Ru–S(7)	88.07(4)	C(5M)–C(6M)–S(7)	112.4(4)
S(4)–Ru–S(7)	88.27(4)	Ru–S(7)–C(6M)	105.42(18)
Ru–S(1)–C(2M)	102.62(19)	Ru–S(7)–C(8M)	102.24(19)
Ru–S(1)–C(9M)	105.87(18)	C(6M)–S(7)–C(8M)	101.3(3)
C(2M)–S(1)–C(9M)	101.1(3)	S(7)–C(8M)–C(9M)	113.9(4)
S(1)–C(2M)–C(3M)	115.1(4)	S(1)–C(9M)–C(8M)	111.5(4)
C(2M)–C(3M)–S(4)	112.4(4)	O–S–C(1)	108.6(4)
Ru–S(4)–C(3M)	105.90(19)	O–S–C(2)	106.7(4)
Ru–S(4)–C(5M)	102.31(19)	C(1)–S–C(2)	98.3(4)
C(3M)–S(4)–C(5M)	102.4(3)		

C(9M)–S(1)–C(2M)–C(3M)	67.7(5)
C(2M)–S(1)–C(9M)–C(8M)	−134.7(4)
S(1)–C(2M)–C(3M)–S(4)	44.9(5)
C(2M)–C(3M)–S(4)–C(5M)	−131.2(4)
C(3M)–S(4)–C(5M)–C(6M)	67.8(4)
S(4)–C(5M)–C(6M)–S(7)	46.5(5)
C(5M)–C(6M)–S(7)–C(8M)	−132.5(4)
C(6M)–S(7)–C(8M)–C(9M)	65.7(4)
S(7)–C(8M)–C(9M)–S(1)	48.3(5)

* M denotes macrocyclic carbon atoms.

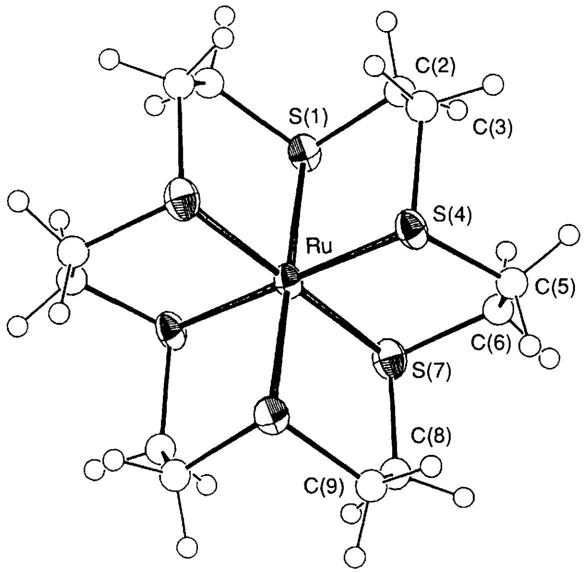

Figure 5. Single crystal *X*-ray structure of $[Ru([18]aneS_6)]^{2+}$ with atom numbering scheme adopted; 30% probability level used for ellipsoids

Table 3. Atomic co-ordinates with e.s.d.s for $[Ru([9]aneS_3)_2][BPh_4]_2 \cdot 2Me_2SO$

Atom	*x*	*y*	*z*
Ru	0.5	0.0	0.5
S(1)	0.428 85(9)	0.065 77(11)	0.396 18(6)
C(2M)	0.338 4(4)	0.168 5(5)	0.421 6(3)
C(3M)	0.285 2(4)	0.126 4(5)	0.480 4(3)
S(4)	0.364 22(9)	0.064 20(12)	0.549 71(6)
C(5M)	0.306 5(4)	−0.077 7(5)	0.567 6(3)
C(6M)	0.308 0(4)	−0.170 6(5)	0.511 8(3)
S(7)	0.425 82(9)	−0.185 74(10)	0.479 41(6)
C(8M)	0.395 9(4)	−0.180 8(5)	0.387 7(3)
C(9M)	0.355 9(4)	−0.060 4(5)	0.362 3(3)
S	0.034 38(11)	−0.124 06(16)	0.389 84(9)
O	0.120 6(3)	−0.065 5(5)	0.424 1(3)
C(1)	0.061 8(6)	−0.272 3(8)	0.371 5(5)
C(2)	−0.042 2(5)	−0.151 5(9)	0.452 1(4)
B	0.723 2(4)	0.023 3(5)	0.858 1(3)
C(11)	0.730 97(22)	−0.006 1(3)	0.942 44(11)
C(12)	0.817 62(22)	−0.042 3(3)	0.974 74(11)
C(13)	0.826 44(22)	−0.059 3(3)	1.044 91(11)
C(14)	0.748 59(22)	−0.040 1(3)	1.082 85(11)
C(15)	0.661 94(22)	−0.003 8(3)	1.050 55(11)
C(16)	0.653 12(22)	0.013 2(3)	0.980 37(11)
C(21)	0.778 23(20)	0.156 70(22)	0.842 42(15)
C(22)	0.744 13(20)	0.227 90(22)	0.787 61(15)
C(23)	0.793 63(20)	0.331 05(22)	0.770 78(15)
C(24)	0.877 25(20)	0.362 99(22)	0.808 76(15)
C(25)	0.911 35(20)	0.291 78(22)	0.863 61(15)
C(26)	0.861 86(20)	0.188 64(22)	0.880 41(15)
C(31)	0.777 73(22)	−0.085 76(23)	0.816 79(15)
C(32)	0.826 85(22)	−0.059 00(23)	0.760 06(15)
C(33)	0.843 67(22)	−0.151 83(23)	0.722 93(15)
C(34)	0.853 37(22)	−0.271 44(23)	0.742 53(15)
C(35)	0.804 23(22)	−0.298 19(23)	0.799 21(15)
C(36)	0.766 40(22)	−0.205 36(23)	0.836 36(15)
C(41)	0.607 24(16)	0.027 45(24)	0.828 01(15)
C(42)	0.554 80(16)	0.133 11(24)	0.833 10(15)
C(43)	0.461 01(16)	0.138 28(24)	0.805 34(15)
C(44)	0.419 70(16)	0.037 77(24)	0.772 49(15)
C(45)	0.472 15(16)	−0.067 90(24)	0.767 40(15)
C(46)	0.565 90(16)	−0.073 05(24)	0.795 16(15)

recorded at 200.13 and 50.32 MHz respectively on a Bruker WP200 spectrometer. Additionally, ^1H n.m.r. spectra were recorded at 360 MHz on a Bruker WH360 spectrometer.

Synthesis of $[Ru([9]aneS_3)_2][BPh_4]_2$.—The compound $[\{RuCl_2(arene)\}_2]$ (arene = C_6H_6, $4\text{-}MeC_6H_4Pr^i$, or C_6Me_6) (0.05 g) was treated with four molar equivalents of $[9]aneS_3$ in refluxing MeOH (15 cm^3) under N_2 for 2 h. The red colour of the Ru starting material faded to give colourless or pale yellow solutions. Addition of $NaBPh_4$ afforded a white precipitate which was recrystallised from Me_2SO to give $[Ru([9]aneS_3)_2][BPh_4]_2 \cdot 2Me_2SO$ in 60% yield {Found: C, 61.6; H, 6.2. Calc. for $[Ru([9]aneS_3)_2][BPh_4]_2 \cdot 2Me_2SO$ C, 61.2; H, 6.1%}. I.r. spectrum: 1 080 cm^{-1} [ν(S=O)].

Single-crystal Structure Determination of $[Ru([9]aneS_3)_2][BPh_4]_2 \cdot 2Me_2SO$.—A colourless plate (0.54 × 0.33 × 0.08 mm) was obtained by cooling a solution of the complex in Me_2SO.

Crystal data. $C_{60}H_{64}B_2RuS_6 \cdot 2C_2H_6OS$ $M = 1\,256.2$, monoclinic, space group $P2_1/c$, $a = 14.134(3)$, $b = 11.096\,3(19)$, $c = 19.743(4)$ Å, $\beta = 94.497(16)°$, $U = 3\,087$ Å^3 (by least-squares refinement on diffractometer angles for 12 centred reflections, $\lambda = 0.710\,73$ Å, $T = 298$ K), $Z = 2$ (implying that each Ru lies on a crystallographic inversion centre), $D_c = 1.352$ g cm^{-3}, $\mu(Mo\text{-}K_\alpha) = 0.55$ mm^{-1}, $F(000) = 1\,316$.

Data collection and processing. Stoë STADI-4 four-circle diffractometer, ω—2θ mode with ω scan width (0.8 + 0.347 tan θ)°, graphite monochromated Mo-K_α radiation; 4 270 reflections measured ($2\theta_{max.}$ 45°, h −15 to 15, k 0—11, l 0—21), giving 2 936 with $F \geqslant 6\sigma(F)$, no absorption correction, no crystal decay.

Structure analysis and refinement. After analysis of intensity statistics showed the Ru to lie on a crystallographic inversion

Table 4. Bond lengths (Å), angles and torsion angles (°) with e.s.d.s for $[Ru([9]aneS_3)_2][BPh_4]_2{\cdot}2MeNO_2$*

Ru–S(1)	2.338 8(17)	S(4)–C(5M)	1.807(8)
Ru–S(4)	2.336 3(16)	C(5M)–C(6M)	1.497(11)
Ru–S(7)	2.330 8(17)	C(6M)–S(7)	1.866(8)
S(1)–C(2M)	1.831(7)	S(7)–C(8M)	1.811(8)
C(2M)–C(3M)	1.523(10)	C(8M)–C(9M)	1.497(11)
C(3M)–S(4)	1.833(7)	C(9M)–S(1)	1.823(8)
S(1)–Ru–S(4)	87.74(6)	Ru–S(4)–C(5M)	102.3(3)
S(1)–Ru–S(7)	87.65(6)	C(3M)–S(4)–C(5M)	102.3(3)
S(4)–Ru–S(7)	87.94(6)	S(4)–C(5M)–C(6M)	114.1(5)
Ru–S(1)–C(2M)	101.93(24)	C(5M)–C(6M)–S(7)	111.9(5)
Ru–S(1)–C(9M)	105.4(3)	Ru–S(7)–C(6M)	104.90(25)
C(2M)–S(1)–C(9M)	101.3(3)	Ru–S(7)–C(8M)	102.8(3)
S(1)–C(2M)–C(3M)	113.4(5)	C(6M)–S(7)–C(8M)	101.0(4)
C(2M)–C(3M)–S(4)	111.1(5)	S(7)–C(8M)–C(9M)	114.7(6)
Ru–S(4)–C(3M)	105.98(23)	S(1)–C(9M)–C(8M)	112.4(6)

C(9M)–S(1)–C(2M)–C(3M)	63.8(6)
C(2M)–S(1)–C(9M)–C(8M)	−133.6(6)
S(1)–C(2M)–C(3M)–S(4)	49.7(6)
C(2M)–C(3M)–S(4)–C(5M)	−135.3(5)
C(3M)–S(4)–C(5M)–C(6M)	65.0(6)
S(4)–C(5M)–C(6M)–S(7)	48.2(7)
C(5M)–C(6M)–S(7)–C(8M)	−132.9(6)
C(6M)–S(7)–C(8M)–C(9M)	67.2(6)
S(7)–C(8M)–C(9M)–S(1)	46.9(7)

* M denotes macrocyclic carbon atoms.

Table 5. Atomic co-ordinates with e.s.d.s for $[Ru([9]aneS_3)_2][BPh_4]_2{\cdot}2MeNO_2$

Atom	*x*	*y*	*z*
Ru	0.5	0.5	0.5
S(1)	0.477 41(14)	0.574 96(10)	0.368 49(11)
C(2M)	0.628 8(6)	0.575 5(4)	0.321 8(5)
C(3M)	0.725 4(6)	0.586 7(4)	0.396 4(4)
S(4)	0.704 74(13)	0.523 85(10)	0.494 73(11)
C(5M)	0.727 4(6)	0.583 3(5)	0.594 3(5)
C(6M)	0.635 2(7)	0.642 2(4)	0.603 3(5)
S(7)	0.480 53(15)	0.605 12(10)	0.590 98(12)
C(8M)	0.415 0(7)	0.670 2(4)	0.509 8(6)
C(9M)	0.465 6(7)	0.668 0(4)	0.413 7(6)
B	−0.047 1(6)	0.272 4(4)	0.412 9(4)
C(11)	0.073 6(3)	0.220 39(21)	0.437 1(3)
C(12)	0.147 5(3)	0.236 39(21)	0.513 6(3)
C(13)	0.250 7(3)	0.195 32(21)	0.529 8(3)
C(14)	0.280 1(3)	0.138 26(21)	0.469 6(3)
C(15)	0.206 2(3)	0.122 22(21)	0.393 1(3)
C(16)	0.103 0(3)	0.163 29(21)	0.376 8(3)
C(21)	−0.079 2(3)	0.319 41(19)	0.511 14(21)
C(22)	−0.037 1(3)	0.390 91(19)	0.521 86(21)
C(23)	−0.055 6(3)	0.428 48(19)	0.605 25(21)
C(24)	−0.116 2(3)	0.394 54(19)	0.677 90(21)
C(25)	−0.158 2(3)	0.323 02(19)	0.667 20(21)
C(26)	−0.139 7(3)	0.285 46(19)	0.583 80(21)
C(31)	−0.021 5(3)	0.329 40(20)	0.323 15(23)
C(32)	−0.101 0(3)	0.386 98(20)	0.306 66(23)
C(33)	−0.084 9(3)	0.433 33(20)	0.230 41(23)
C(34)	0.010 7(3)	0.422 06(20)	0.170 62(23)
C(35)	0.090 1(3)	0.364 46(20)	0.187 11(23)
C(36)	0.074 0(3)	0.318 13(20)	0.263 36(23)
C(41)	−0.164 9(3)	0.217 22(20)	0.382 8(3)
C(42)	−0.248 0(3)	0.238 60(20)	0.314 6(3)
C(43)	−0.349 5(3)	0.196 07(20)	0.297 7(3)
C(44)	−0.368 0(3)	0.132 18(20)	0.349 0(3)
C(45)	−0.284 9(3)	0.110 79(20)	0.417 1(3)
C(46)	−0.183 4(3)	0.153 31(20)	0.434 0(3)
N(1)	0.478 5(8)	0.425 2(5)	0.159 9(5)
O(1)	0.569 7(8)	0.440 3(5)	0.117 0(5)
O(2)	0.453 4(8)	0.360 7(5)	0.175 2(5)
C(1)	0.420 1(8)	0.482 4(5)	0.213 8(5)
N(1′)	0.478 5(8)	0.425 2(5)	0.159 9(5)
O(1′)	0.377 1(8)	0.437 1(5)	0.188 6(5)
O(2′)	0.532 2(8)	0.369 4(5)	0.184 3(5)
C(1′)	0.520 4(8)	0.465 7(5)	0.0786(5)

centre. DIRDIF[20] located the remaining non-solvent, non-hydrogen atoms. Successive least-squares cycles and difference Fourier syntheses[21] yielded the positions of the solvent atoms. Full-matrix least-squares with idealised phenyl rings for BPh_4^-, H-atoms in calculated positions and anisotropic thermal parameters for Ru, S, O, C, and B atoms converged to R, R' = 0.0431, 0.0590 for 322 parameters and the final ΔF synthesis showed a maximum peak and minimum trough of +0.65 and −0.5 e $Å^{-3}$ respectively. The weighting scheme $w^{-1} = \sigma^2(F) + 0.000\,435F^2$ gave satisfactory agreement analysis. Bond lengths, angles, torsion angles, and fractional atomic co-ordinates are given in Tables 2 and 3 respectively.

Recrystallisation of $[Ru([9]aneS_3)_2][BPh_4]_2$ from MeCN or $MeNO_2$ afforded crystals of the corresponding disolvate {Found: C, 65.1; H, 6.1; N, 2.4. Calc. for $[Ru([9]aneS_3)_2][BPh_4]_2{\cdot}2MeCN$: C, 65.0; H, 6.0; N, 2.4%). I.r. spectrum (KBr disc) 2 243 cm^{-1} [ν(CN)] {Found: C, 61.0; H, 5.75; N, 2.30. Calc. for $[Ru([9]aneS_3)_2][BPh_4]_2{\cdot}2MeNO_2$: C, 60.9; H, 5.75; N, 2.30%}. I.r. spectrum (KBr disc): 2 920 [$\nu(CH_2)$], 1 436 [$\delta(CH_2)$], 1 554, and 1 373 cm^{-1} [$\nu(NO_2)$]; other bands: 3 055, 2 985, 1 578, 1 478, 1 444, 1 429, 1 405, 1 265, 1 171, 1 129, 1 062, 1 031, 935, 905, 845, 831, 752, 735, 705, 658, 610, 468, and 330 cm^{-1}. N.m.r. [$(CD_3)_2SO$, 298 K]: ^1H (200.13 MHz), δ 6.8—7.2 (m, 40 H, BPh_4^-), 4.3 (s, 6 H, CH_3NO_2), 2.9 (CH_2, ABCD, CH_2 of [9]aneS_3); ^{13}C (50.32 MHz), δ 33.34 p.p.m. (CH_2 of [9]aneS_3).

Single-crystal Structure Determination of $[Ru([9]aneS_3)_2][BPh_4]_2{\cdot}2MeNO_2$.—Colourless columnar crystals were obtained by cooling a $MeNO_2$ solution of the complex. Unlike those for $[Ru([9]aneS_3)_2][BPh_4]_2{\cdot}2Me_2SO$, the faces of these crystals degraded on extended exposure to the atmosphere *via* loss of solvent. To maintain crystal integrity during data collection, a crystal (0.31 × 0.46 × 1.16 mm) was encapsulated in a capillary tube with a small portion of mother liquor.

Crystal data. $C_{60}H_{64}B_2RuS_6{\cdot}2C_2H_6NO_2$, M = 1 252.4, monoclinic, space group $P2_1/n$, a = 11.200(5), b = 18.247(13), c = 14.323(17) Å, β = 90.78(4)°, U = 2 927 $Å^3$ (by least-squares refinement on diffractometer angles for 20 centred reflections, λ = 0.710 73 Å, T = 298 K), Z = 2 (implying that each Ru centre lies on a crystallographic inversion centre), D_c = 1.421 g cm^{-3}, $\mu(Mo\text{-}K_\alpha)$ = 0.516 mm^{-1}, $F(000)$ = 1 312.

Data collection and processing. Stoë STADI-4 four-circle diffractometer, ω—θ mode with ω scan width (0.875 + 0.347 tan θ)°, graphite monochromated Mo-K_α radiation; 5 551 reflections measured ($2.5 \leqslant \theta \leqslant 22.5°$, h −13 to 13, k 0—20, l 0—16), giving 3 759 with $F \geqslant 6\sigma(F)$, no absorption correction, no crystal decay.

Structure analysis and refinement. Intensity statistics indicated the position of the Ru atom on an inversion centre and from this starting point DIRDIF[20] located all remaining non-solvent and non-hydrogen atoms. Successive cycles of least-squares refinement and difference Fourier synthesis[21] yielded the positions of the solvent atoms. At isotropic convergence corrections for absorption were applied using DIFABS.[22] Full-matrix least-squares with idealised phenyl rings for BPh_4^-, H-atoms in calculated positions and anisotropic thermal parameters for Ru, S, C, and B atoms and idealised nitromethane molecules disordered over two positions. The weighting scheme

Table 6. Bond lengths (Å), angles and torsion angles (°) with e.s.d.s for $[Ru([18]aneS_6)][BPh_4]_2$

Ru–S(1)	2.322 2(23)	S(4)–C(5)	1.840(11)
Ru–S(4)	2.332 6(25)	C(5)–C(6)	1.509(14)
Ru–S(7)	2.337 2(23)	C(6)–S(7)	1.825(10)
S(1)–C(2)	1.806(10)	S(7)–C(8)	1.816(9)
C(2)–C(3)	1.520(14)	C(8)–C(9)	1.519(13)
C(3)–S(4)	1.828(11)	C(9)–S(1′)	1.826(10)
S(1)–Ru–S(4)	88.67(8)	Ru–S(4)–C(5)	105.0(3)
S(1)–Ru–S(7)	91.61(8)	C(3)–S(4)–C(5)	104.1(5)
S(4)–Ru–S(7)	88.54(6)	S(4)–C(5)–C(6)	115.4(7)
Ru–S(1)–C(2)	105.5(3)	C(5)–C(6)–S(7)	114.2(7)
Ru–S(1)–C(9′)	103.9(3)	Ru–S(7)–C(6)	104.1(3)
C(2)–S(1)–C(9′)	104.4(5)	Ru–S(7)–C(8)	105.4(3)
S(1)–C(2)–C(3)	115.3(7)	C(6)–S(7)–C(8)	103.9(4)
C(2)–C(3)–S(4)	114.1(7)	S(7)–C(8)–C(9)	114.7(6)
Ru–S(4)–C(3)	103.4(3)	C(8)–C(9)–S(1′)	114.2(7)

C(9′)–S(1)–C(2)–C(3)	−84.8(8)
C(2)–S(1)–C(9′)–C(8′)	73.9(8)
S(1)–C(2)–C(3)–S(4)	−41.1(10)
C(2)–C(3)–S(4)–C(5)	−74.0(8)
C(3)–S(4)–C(5)–C(6)	84.5(8)
S(4)–C(5)–C(6)–S(7)	40.6(9)
C(5)–C(6)–S(7)–C(8)	74.5(8)
C(6)–S(7)–C(8)–C(9)	−84.6(7)
S(7)–C(8)–C(9)–S(1′)	−41.7(9)

Table 7. Atomic co-ordinates with e.s.d.s for $[Ru([18]aneS_6)][BPh_4]_2$

Atom	*x*	*y*	*z*
Ru	0.0	0.0	0.0
S(1)	0.039 34(19)	−0.006 85(22)	−0.105 16(10)
C(2)	0.183 6(8)	−0.049 4(10)	−0.080 7(5)
C(3)	0.229 4(9)	−0.120 5(10)	−0.011 5(5)
S(4)	0.181 64(21)	−0.061 63(22)	0.059 23(12)
C(5)	0.258 5(9)	0.085 7(9)	0.086 7(5)
C(6)	0.208 1(8)	0.199 6(9)	0.043 5(5)
S(7)	0.057 95(21)	0.208 67(19)	0.019 22(11)
C(8)	0.035 2(8)	0.253 9(8)	0.100 8(4)
C(9)	0.034 4(8)	0.145 7(9)	0.149 9(5)
B	0.747 2(9)	0.549 1(9)	0.115 1(5)
C(11)	0.742 7(5)	0.491 4(5)	0.035 03(21)
C(12)	0.641 8(5)	0.448 2(5)	−0.010 82(21)
C(13)	0.634 4(5)	0.404 2(5)	−0.077 81(21)
C(14)	0.728 0(5)	0.403 4(5)	−0.098 96(21)
C(15)	0.828 9(5)	0.446 7(5)	−0.053 12(21)
C(16)	0.836 2(5)	0.490 7(5)	0.013 87(21)
C(21)	0.682 8(5)	0.449 4(5)	0.155 4(3)
C(22)	0.641 8(5)	0.493 5(5)	0.207 5(3)
C(23)	0.590 9(5)	0.410 8(5)	0.241 3(3)
C(24)	0.581 1(5)	0.284 1(5)	0.223 0(3)
C(25)	0.622 1(5)	0.240 1(5)	0.170 8(3)
C(26)	0.672 9(5)	0.322 7(5)	0.137 0(3)
C(31)	0.683 4(4)	0.688 5(4)	0.105 9(3)
C(32)	0.700 5(4)	0.761 2(4)	0.166 4(3)
C(33)	0.640 2(4)	0.871 3(4)	0.163 1(3)
C(34)	0.562 9(4)	0.908 9(4)	0.099 2(3)
C(35)	0.545 9(4)	0.836 2(4)	0.038 6(3)
C(36)	0.606 2(4)	0.726 0(4)	0.041 9(3)
C(41)	0.880 9(4)	0.563 4(5)	0.163 2(3)
C(42)	0.938 5(4)	0.461 3(5)	0.201 4(3)
C(43)	1.053 1(4)	0.467 3(5)	0.232 8(3)
C(44)	1.110 1(4)	0.575 4(5)	0.225 9(3)
C(45)	1.052 5(4)	0.677 5(5)	0.187 6(3)
C(46)	0.937 9(4)	0.671 5(5)	0.156 2(3)

$w^{-1} = \sigma^2(F) + 0.000\,4381F^2$ gave satisfactory agreement analysis. Final R and R' are 0.0691, 0.1005 for 277 parameters and the final ΔF synthesis showed a maximum peak and minimum trough of +1.14 and −1.11 e Å^{-3} respectively. Bond lengths, angles, torsion angles, and fractional atomic co-ordinates are given in Tables 4 and 5 respectively.

Synthesis of $[Ru([9]aneS_3)_2][ClO_4]_2{\cdot}H_2O$.—Hydrated ruthenium trichloride, $RuCl_3{\cdot}3H_2O$ (0.1 g, 0.32 mmol), was dissolved in Me_2SO (15 cm^3) at 180 °C. The solution was concentrated to 7 cm^3 and cooled to 20 °C, and $[9]aneS_3$ (0.22 g, 1.2 mmol) was added. The reaction mixture was heated to 140 °C for 3 h; on cooling to room temperature a white solid precipitated. This product was dissolved in water and recrystallised by addition of $NaClO_4$ {Found: C, 22.7; H, 3.9; S, 28.4. Calc. for $[Ru([9]aneS_3)_2][ClO_4]_2{\cdot}H_2O$: C, 21.2; H, 3.9; S, 28.4%}. Electronic spectrum: $\lambda_{max.}$ ($\varepsilon_{max.}$) = 341 (160), 293 (183), and 220 nm (20 040 dm^3 mol^{-1} cm^{-1}); ^1H n.m.r. [80 MHz, $(CD_3)_2SO$, 293 K]: δ 2.90 (s, CH_2), in D_2O δ 2.78 (s). The complex $[Ru([9]aneS_3)_2][PF_6]_2$ can be prepared by similar routes either from $RuCl_3$ or from $[\{RuCl_2(arene)\}_2]$ {Found: C, 19.4; H, 3.20. Calc. for $[Ru([9]aneS_3)_2][PF_6]_2$: C, 19.2; H, 3.20%}. F.a.b. mass spectrum (dmf–glycerol): *m*/*z* 607 and 461; calc. for $[Ru([9]aneS_3)_2PF_6]^+$ 607, $[Ru([9]aneS_3)_2 - H]^+$ 461 with correct isotopic distributions.

Synthesis of $[Ru([18]aneS_6)][PF_6]_2$.—Reaction of $RuCl_3{\cdot}3H_2O$ (0.12 g, 0.46 mmol) and $[18]aneS_6$ (0.2 g, 0.56 mmol) in refluxing dmf–MeOH (20 cm^3, 10:1 v/v) under N_2 for 2 h afforded $[Ru([18]aneS_6)]Cl_2$ as a white precipitate which was collected from the cooled solution and washed with MeOH, CH_2Cl_2, and finally Et_2O. The product was dissolved in hot H_2O (30 cm^3). Addition of an excess of NH_4PF_6 gave a white precipitate of $[Ru([18]aneS_6)][PF_6]_2$ which was recrystallised by vapour diffusion of CH_2Cl_2 into a solution of the complex in Me_2SO: Yield 63% (Found: C, 19.3; H, 3.30. Calc. for $[Ru([18]aneS_6)][PF_6]_2$: C, 19.2; H, 3.25%). I.r. spectrum (KBr disc): 2 985, 2 940, 1 430, 1 408, 1 325, 1 280, 1 175, 1 132, 1 080, 1 024, 950, 840, 620, 556, and 495 cm^{-1}. F.a.b. mass spectrum [3-nitrobenzyl alcohol (noba) matrix]: *m*/*z* 607, 461; calc. for $[Ru([18]aneS_6)PF_6]^+$ 607, $[Ru([18]aneS_6) - H]^+$ 461 with correct isotopic distributions. Electronic spectrum (Me_2SO): $\lambda_{max.}$ ($\varepsilon_{max.}$) = 352.6 (125), 282.4 nm (293 dm^3 mol^{-1} cm^{-1}). The complex $[Ru([18]aneS_6)][PF_6]_2$ is insoluble in all common organic solvents except Me_2SO.

Synthesis of $[Ru([18]aneS_6)][BPh_4]_2{\cdot}2MeNO_2$.—Hydrated ruthenium trichloride, $RuCl_3{\cdot}3H_2O$ (0.08 g, 0.3 mmol), was treated with $[18]aneS_6$ (0.13 g, 0.36 mmol) in refluxing dmf–MeOH (15 cm^3, 10:1 v/v) for 2 h under N_2; $NaBPh_4$ (0.4 g, 1.17 mmol) in H_2O (15 cm^3) was added and the reaction mixture refluxed for a further 1 h. Addition of H_2O (20 cm^3) and cooling afforded a white precipitate which was collected and recrystallised from $MeNO_2$ to afford $[Ru([18]aneS_6)][BPh_4]_2{\cdot}2MeNO_2$ in 22% yield (Found: C, 60.9; H, 5.75; N, 2.30. Calc. for $[Ru([18]aneS_6)][BPh_4]_2{\cdot}2MeNO_2$: C, 60.9; H, 5.75; N, 2.25%). F.a.b. mass spectrum (noba matrix): *m*/*z* 781 and 461; calc. for $[Ru([18]aneS_6)(BPh_4)]^+$ 781, $[Ru([18]aneS_6) - H]^+$ 461. Proton n.m.r. [360.13 MHz, $(CD_3)_2SO$, 333 K]: δ 7.22 (m, 16 H), 6.93 (m, 16 H), 6.80 (m, 8 H) (BPh_4^-), 4.40 (s, CH_3NO_2, 6 H), and 2.96 (CH_2, AA′BB′, 24 H); ^{13}C n.m.r. [50.32 MHz, $(CD_3)_2SO$, 298 K]: δ 38.57 p.p.m. (CH_2 of co-ordinated $[18]aneS_6$).

Single-crystal Structure Determination of $[Ru([18]aneS_6)][BPh_4]_2$.—A colourless lath (0.462 × 0.173 × 0.08 mm) was grown by vapour diffusion of MeOH into a solution of the complex in Me_2SO.

Crystal data. $C_{60}H_{64}B_2RuS_6$, M = 1 100.2, monoclinic, space group $P2_1/c$, a = 12.801(4), b = 10.663(3), c = 20.036(9) Å, β = 109.09(3)°, U = 2 584 Å^3 [from 2θ values of 38 reflections measured at $\pm\omega(2\theta = 20$—$25°$, λ = 0.710 73 Å, $T = 223 \pm 0.2$ K), Z = 2 (implying that the Ru lies on a crystallographic inversion centre), D_c = 1.414 g cm^{-3}, μ = 0.569 mm^{-1}, F(000) = 1 148.

Data collection and processing. Stoë STADI-4 four-circle diffractometer equipped with Oxford Cryosystems low-temperature device,[23] graphite monochromated Mo-K_α X-radiation, T = 223 K, ω—2θ scans using the learnt-profile method,[24] 3 693 data measured ($2\theta_{max.}$ 45°; $\pm h$, $+k$, $+l$), 3 196 unique (R_{int} = 0.032), yielding 1 915 with $F \geqslant 6\sigma(F)$ for use in all calculations. Slight isotropic crystal decay (*ca.* 10%) corrected for during data reduction.

Structure solution and refinement. From the Ru position suggested by cell contents and intensity statistics, successive cycles of least-squares refinement and difference Fourier synthesis located all non-H atoms: these were then refined (by least-squares on F[21]) with anisotropic thermal parameters. Hydrogen atoms were included at fixed, calculated positions. At final convergence R, R' = 0.0521, 0.0638 respectively, S = 1.058 for 265 refined parameters and in the final ΔF synthesis no peak was above 0.69 e Å^{-3}. The weighting scheme $w^{-1} = \sigma^2(F) + 0.000\,775F^2$ gave satisfactory agreement analysis and in the final cycle $(\Delta/\sigma)_{max.}$ was 0.023. Bond lengths, angles, torsion angles, and fractional co-ordinates are given in Tables 6 and 7 respectively.

Atomic scattering factors were inlaid,[21] or taken from ref. 25. Molecular geometry calculations utilised CALC[26] and the Figures were produced by ORTEPII.[27]

Additional material available from the Cambridge Crystallographic Data Centre comprises H-atom co-ordinates, thermal parameters, and remaining bond lengths and angles.

Acknowledgements

We thank the University of Edinburgh (to M.N.B.) and the S.E.R.C. for support. We are grateful to Johnson-Matthey for generous loans of platinum metals, and thank Professor Karl Wieghardt and Dr. Heinz Küppers for helpful discussions.

References

1 A. J. Blake and M. Schröder, *Adv. Inorg. Chem.*, 1990, **35**, 1; M. Schröder, *Pure Appl. Chem.*, 1988, **60**, 517; M. N. Bell, A. J. Blake, R. O. Gould, A. J. Holder, T. I. Hyde, A. J. Lavery, G. Reid, and M. Schröder, *J. Inclusion Phenom.*, 1987, **5**, 169.

2 W. N. Setzer, C. A. Ogle, G. S. Wilson, and R. S. Glass, *Inorg. Chem.*, 1983, **22**, 266.

3 M. N. Bell, A. J. Blake, H-J. Küppers, M. Schröder, and K. Wieghardt, *Angew. Chem.*, 1987, **99**, 253; *Angew. Chem. Int. Ed. Engl.*, 1987, **26**, 250.

4 S. C. Rawle and S. R. Cooper, *J. Chem. Soc., Chem. Commun.*, 1987, 308; S. C. Rawle, T. J. Sewell, and S. R. Cooper, *Inorg. Chem.*, 1987, **26**, 3769.

5 D. St. C. Black and I. A. McLean, *Tetrahedron Lett.*, 1969, 3961; *Aust. J. Chem.*, 1971, **24**, 1401; S. R. Cooper, *Acc. Chem. Res.*, 1988, **21**, 141.

6 A. J. Blake, R. O. Gould, A. J. Lavery, and M. Schröder, *Angew. Chem.*, 1986, **98**, 282; *Angew. Chem. Int. Ed. Engl.*, 1986, **25**, 274.

7 A. J. Blake, R. O. Gould, A. J. Holder, T. I. Hyde, A. J. Lavery, G. Reid, and M. Schröder, unpublished work.

8 A. J. Blake, R. O. Gould, A. J. Holder, T. I. Hyde, and M. Schröder, *Polyhedron*, 1989, **8**, 513.

9 A. J. Blake, R. O. Gould, J. A. Greig, A. J. Holder, T. I. Hyde, and M. Schröder, *J. Chem. Soc., Chem. Commun.*, 1989, 876; A. J. Blake, J. A. Greig, A. J. Holder, T. I. Hyde, A. Taylor, and M. Schröder, *Angew. Chem.*, 1990, **102**, 203; *Angew. Chem. Int. Ed. Engl.*, 1990, **29**, 197.

10 A. J. Blake, R. O. Gould, A. J. Holder, T. I. Hyde, and M. Schröder, *J. Chem. Soc., Dalton Trans.*, 1988, 1861.

11 H-J. Küppers, A. Neves, C. Pomp, D. Ventur, K. Wieghardt, B. Nuber, and J. Weiss, *Inorg. Chem.*, 1986, **25**, 2400; G. S. Wilson, D. D. Swanson, and R. S. Glass, *ibid.*, 1986, **25**, 3827.

12 K. Wieghardt, H-J. Küppers, and J. Weiss, *Inorg. Chem.*, 1985, **24**, 3067.

13 H-J Küppers, K. Wieghardt, B. Nuber, J. Weiss, E. Bill, and A. X. Trautwein, *Inorg. Chem.*, 1987, **26**, 3762; A. J. Blake, A. J. Holder, T. I. Hyde, and M. Schröder, *J. Chem. Soc., Chem. Commun.*, 1989, 1433.

14 R. M. Christie, M. N. Bell, A. J. Blake, A. J. Holder, M. Schröder, and L. J. Yellowlees, unpublished work.

15 A. J. Blake, R. O. Gould, A. J. Holder, T. I. Hyde, G. Reid, and M. Schröder, *J. Chem. Soc., Dalton Trans.*, 1990, 1759.

16 A. J. Blake, A. J. Holder, T. I. Hyde, and M. Schröder, *J. Chem. Soc., Chem. Commun.*, 1987, 987.

17 A. J. Blake, R. O. Gould, A. J. Holder, T. I. Hyde, M. O. Odulate, A. J. Lavery, and M. Schröder, *J. Chem. Soc., Chem. Commun.*, 1987, 118.

18 A. J. Blake, A. J. Holder, T. I. Hyde, H-J. Küppers, M. Schröder, and K. Wieghardt, *J. Chem. Soc., Chem. Commun.*, 1989, 1600.

19 M. Schröder and T. A. Stephenson, 'Comprehensive Coordination Chemistry,' eds. G. Wilkinson, J. A. McCleverty, and R. D. Gillard, Pergamon Press, 1987, vol. 4, p. 277, and refs. therein.

20 DIRDIF, Applications of Direct Methods to Difference Structure Factors, P. T. Beurskens, W. P. Bosman, H. M. Doesbury, Th. E. M. van den Hark, P. A. J. Prick, J. H. Noordik, G. Beurskens, R. O. Gould, and V. Parthasarathai, University of Nijmegen, 1983.

21 SHELX 76, program for crystal structure refinement, G. M. Sheldrick, University of Cambridge, 1976.

22 DIFABS, Program for Empirical Absorption Corrections, N. Walker and D. Stuart, *Acta Crystallogr., Sect. A*, 1983, **39**, 158.

23 J. Cosier and A. M. Glazer, *J. Appl. Crystallogr.*, 1986, **18**, 105.

24 W. Clegg, *Acta Crystallogr., Sect. A*, 1981, **37**, 22.

25 D. T. Cromer and J. L. Mann, *Acta Crystallogr., Sect A*, 1968, **24**, 321.

26 CALC, program for molecular geometry calculations, R. O. Gould and P. Taylor, University of Edinburgh, 1985.

27 ORTEPII, interactive version, P. D. Mallinson and K. W. Muir, *J. Appl. Crystallogr.*, 1985, **18**, 51.

Received 21*st May* 1990; *Paper* 0/02227D